Preliminary Mapping of Surface Fault Rupture and Ground Deformation Features of the 2019 M6.4 and M7.1 Ridgecrest Earthquake Sequence from Post-Earthquake Lidar and Orthoimagery Datasets

Carla M. Rosa, Reva Kakaria, and Timothy E. Dawson
California Geological Survey, San Mateo, California

California Department of Conservation
California Geological Survey

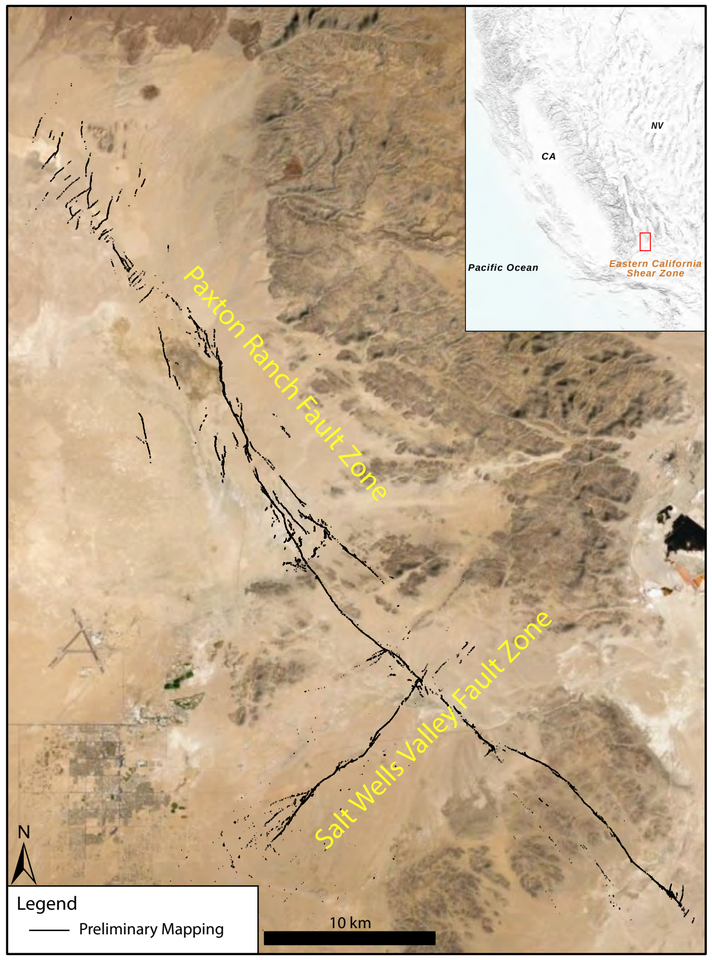

Abstract

We present preliminary mapping of surface ruptures and ground-deformation features associated with the 2019 Ridgecrest Earthquake Sequence. The mapping utilizes high-resolution airborne lidar and orthoimagery acquired post-earthquake by the National Center for Airborne Laser Mapping (Hudnut et al., 2020). The MW 6.4 and MW 7.1 earthquakes produced rupture and ground deformation zones approximately 18 km and 50 km in length, respectively, with widespread deformation occurring off the main fault strands. Our goal is to produce a comprehensive and spatially accurate dataset depicting surface ruptures associated with the Salt Wells Valley and Paxton Ranch Fault Zones. We used seamless lidar-derived hillshades, illuminated at 45- and 315-degrees, and supplemented with a multi-directional hillshade as the base imagery. Mapping on the lidar was done at a consistent (1:500 – 1:1000) scale, the largest scale at which imagery resolution is not degraded. Use of this large scale increases our confidence that we have only mapped features that are related to ground deformation from the earthquake. Features on the orthoimagery were mapped at a larger scale (~1:300), allowing for finer-scale features to be resolved. The surface rupture was mapped to highlight the width of deformation zones and to characterize the rupture's expression through varying terrain, such as pre-existing fault scarps, hillslopes, fan surfaces, and relatively flat playa surfaces. Our mapping reliably resolved ruptures with tens of centimeters and more of relative vertical displacement. Areas with known surface rupture but little vertical displacement are less well-resolved on the lidar compared to the orthoimagery. Mapping using orthoimagery is limited by image resolution, variable image quality, and time available to map at a high level of detail. Thus, characterizing zones of deformation for the 2019 Ridgecrest Earthquake Sequence, important for the assessment of fault displacement hazard, appears to require a paired approach using both lidar and high-resolution aerial imagery. Although these datasets do not capture the same level of detail as low-altitude UAV imagery, our mapping is spatially more complete, improves upon previous mapping of areas with inferred surface rupture, and includes ruptures not previously identified in the field, or by preliminary remote sensing.

Methodology

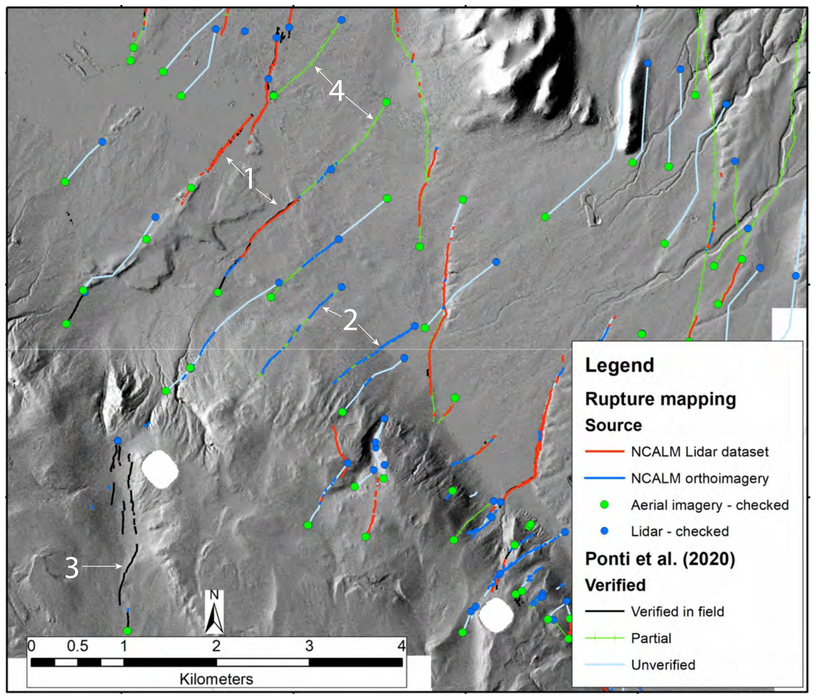

Our methodology includes mapping undetected fault-related features, as well as checks against previously published post-earthquake linework from Ponti et al. (2020), which is currently the most comprehensive published mapping for the 2019 Ridgecrest Earthquake Sequence. Additionally, we also are checking the imagery against previously mapped faults, such as those from the USGS Quaternary fault and fold database.

We created four classes of rupture linework (numbers reference those on image above):

1. Visible on lidar (and generally on orthoimagery)
2. Visible on orthoimagery but not on lidar; these are mostly surface fractures with little vertical displacement
3. Feature verified in the field, on post-earthquake optical imagery, or inferred from multiple observation points, but not visible on imagery to us
4. Feature has one or more site observations along strike, but low confidence as to the overall extent and continuity

If fault-related features are visible on lidar, they are mapped and attributed as lidar-derived. This involves reviewing the three lidar derivatives we are using. Fault-related features visible only on orthoimagery are mapped and attributed as aerial-imagery derived. If no fault-related features are visible on either the lidar or orthoimagery, points are recorded in our database as "checked points."

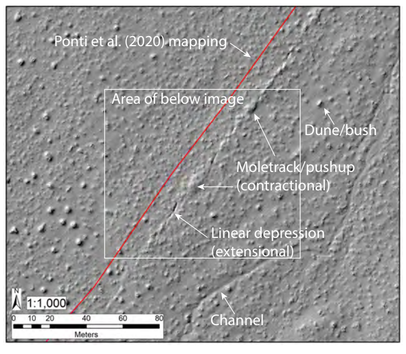

1:1000 scale image:

This image illustrates what is visible to us on the lidar vs. the generalized mapping from Ponti et al. (2020). The lidar provides an opportunity to capture better location accuracy for these faulting-related features. The expression of this earthquake is predominantly characterized by contractional and extensional features, which include moletracks, push ups, and linear depressions.

This image also highlights the landscape of the arid environment we are mapping and how we are differentiating between tectonic and non-tectonic geomorphology, such as channels and dunes.

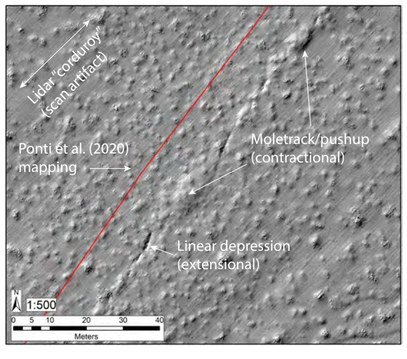

1:500: scale image:

Although lidar artifacts become more noticeable, this scale seems to strike a good balance between being able to resolve rupture features and having an overabundance of artifacts.

In addition to mapping with a higher location accuracy, our methods allow us to qualitatively describe the fault-related features and structures we map, creating an extensive catalog of metadata for these fault zones.

Appearance of Features in Orthoimagery vs. Lidar

Here, features are easily mappable on the lidar. However, those same features are not visible on the orthoimagery, likely due to the sandy nature of the area, making it difficult to view vertical offset.

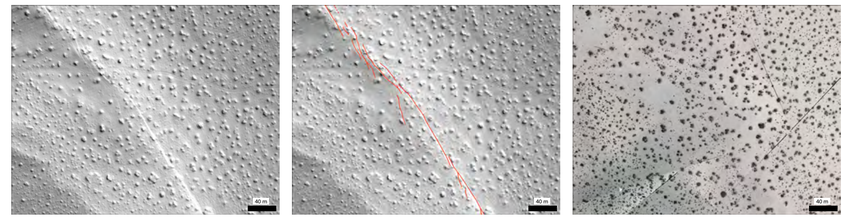

At this location, rupture is not visible on the lidar and lidar artifacts make it hard to reconcile the exact fault location. In the orthoimagery, while discontinuous, the ruptures are visible and are more easily mapped.

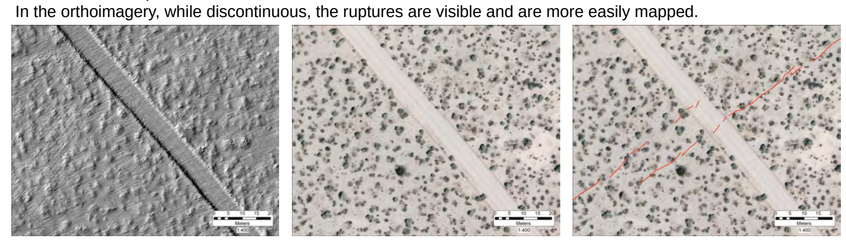

Comparisons with Previous Mapping

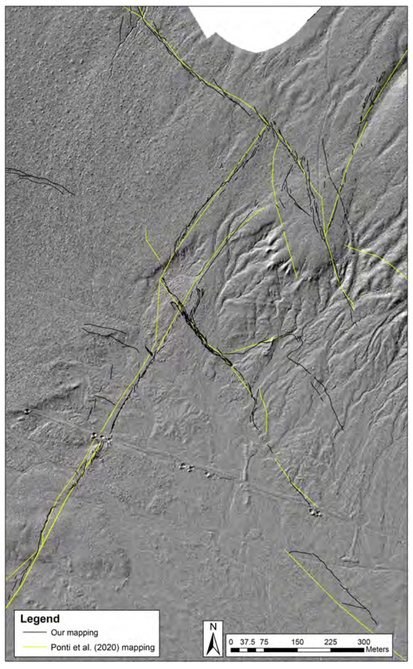

When comparing our mapping against the previously published dataset of Ponti et al. (2020), it is apparent that we have captured many of the same features. However, we generally have better location accuracy, and are able to be more specific with regards to the expression of the ruptures. This previous dataset is a compilation of various sources acquired at various scales; whereas our mapping is internally consistent, utilizing the same source and mapped by all contributors at approximately the same scale.

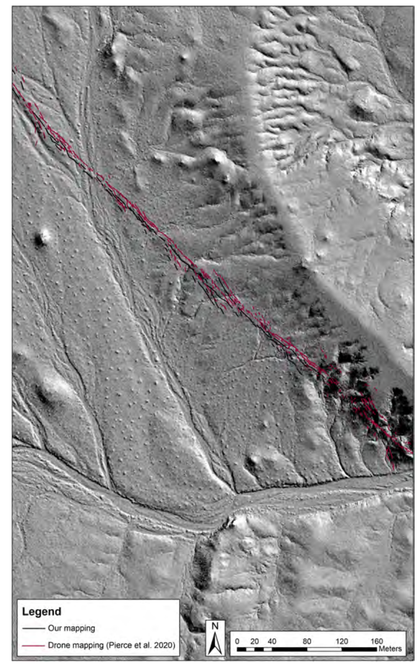

We also compared our mapping with that of Pierce et al. (2020), which is included within the Ponti et al. (2020) dataset. This mapping utilizes low-altitude aerial photographs collected with drones, providing a high resolution dataset for mapping. While we are able to map most features visible to us on the lidar, it does not capture fine-scale features that are visible on the drone images. This demonstrate how low-altitude images are useful for areas with distributed, complex faulting. Trade-offs should be considered with regards to the available person hours for mapping, as well as the base footprint, when choosing a mapping source.

Background and Goals

The Ridgecrest Earthquake Sequence occurred in the summer of 2019 and consisted of two separate earthquake events. These events, located in southeastern California, in the Eastern California Shear Zone, occurred along two orthogonal cross-faults, defining two fault zones.

The first was a magnitude 6.4 event on July 4th, a left-lateral, northeast-striking rupture 18 km long across the Salt Wells Valley Fault Zone. The second, a magnitude 7.1 event in the Paxton Ranch Fault Zone, was right-lateral and northwest striking, with a 50 km-long rupture.

Both fault zones are complex, with multiple fault strands and conjugate faults that often show vertical displacement. The two events also triggered slip along both the Garlock and Little Lake Fault Zones and led to additional surface manifestations, including liquefaction and sand boils in playa areas.

Our goal for this project is to produce an internally consistent, large-scale surface rupture map of the 2019 earthquake ruptures utilizing high-resolution, post-earthquake lidar and orthoimagery from Hudnut, et al. (2020).

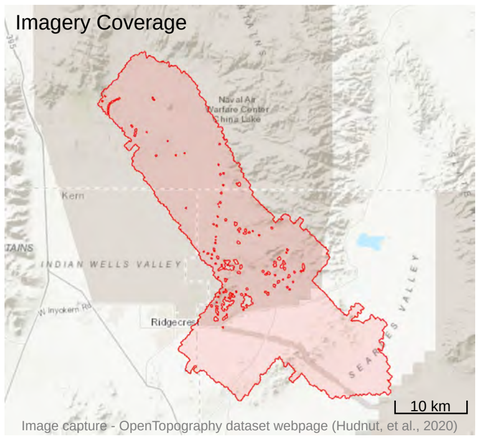

Image capture - OpenTopography dataset webpage (Hudnut, et al., 2020)

We aim to improve upon existing compiled earthquake rupture mapping products (i.e. Ponti et al. 2020). To this end, we are producing a comprehensive and spatially accurate dataset depicting surface ruptures associated with the Salt Wells Valley and Paxton Ranch Fault Zones for use in assessment of fault displacement hazards.

Our final mapping product will provide a basis for Alquist-Priolo earthquake fault zoning in California, as well as contribute to USGS/CGS Quaternary fold and fault databases.

We are using standardized lidar derivative products such as 45°, 315°, and multi-directional hillshades. An example of these hillshades and their differences is shown below.

Lidar Derivatives Used

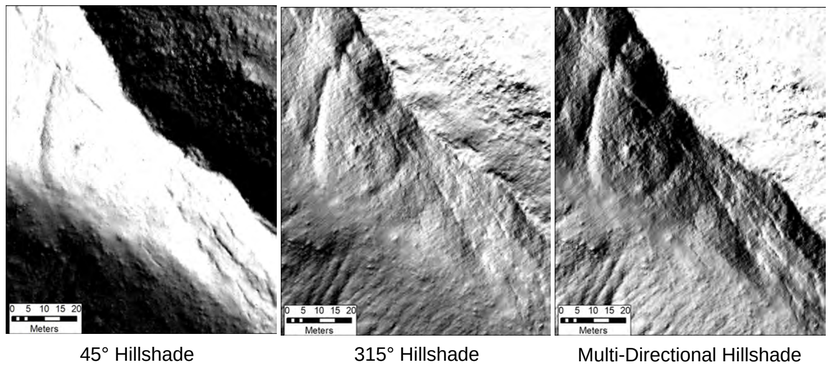

45° Hillshade | 315° Hillshade | Multi-Directional Hillshade

Most of our mapping is done at a 1:500 scale, using a combination of the 45°, 315°, and multi-directional hillshades shown above.

We find the multi-directional hillshade to be very useful in this type of arid, desert environment, as it combines light from six different directions, enhancing the terrain and improving the appearance of regions with low relief. It also balances out the overexposed and shadowed areas of the map.

Based on our experience, we believe these to be standard lidar derivative products that could be used in any future earthquake rupture and ground deformation mapping projects, capturing almost every visible feature.

Conclusions

This lidar and orthoimagery dataset is, thus far, one of the highest resolution, spatially extensive, and complete datasets acquired for post-earthquake rupture mapping. This pairing should always be collected as each type of mapping source has unique advantages. We found that high-resolution lidar imagery easily captures well-defined ruptures with ~20 cm of vertical displacement, and sometimes even less. In areas where width of deformation increases, features are less well-resolved, but in many cases are still identifiable. Utilizing orthoimagery is still necessary for identifying ruptures with little vertical offset and those that are expressed primarily as zones of fractures. The orthoimagery is of variable quality due to blurriness and lighting conditions, but we find that ruptures can be typically resolved at 1:500 scale or larger. The orthoimagery is especially valuable for ruptures with distributed faulting and for verifying significance of deformation recorded using other techniques. Although mapping on the aerial imagery is possible at scales larger than 1:500, practical considerations such as the large area involved and limited person hours make more detailed mapping less feasible.

Our mapping database demonstrates the utility for identifying active faults with slight, long-term geomorphic expression, but that are potentially active within the current tectonic regime. Acquiring detailed mapping of earthquake surface ruptures and other fault-related deformation features allows for better understanding of fault mechanics and potential hazard. The spatial completeness of these data suggests that past ruptures and distributed faulting have been previously incompletely documented.

Future Work

Future work will entail examining in detail the lidar and orthoimagery dataset to better quantify near-field distributed deformation. Additionally, we want to explore the potential to develop models to estimate displacements based on expression of surface rupture. We believe that detailed mapping utilizing high-resolution imagery, such as our dataset, can be used to potentially examine the expression of surface rupture and displacements in geologically variable materials. Our work could also be used in the automation of mapping, specifically as a training dataset for machine learning. This, combined with remote-sensing data, may be a path forward to decrease person-hours involved in detailed mapping.

References

Hudnut, K.W., et al. (2020). Airborne Lidar and Electro-Optical Imagery along Surface Ruptures of the 2019 Ridgecrest Earthquake Sequence, Southern California. Seismological Research Letters 91, 2096-2107, doi: 10.1785/0220190338

Pierce, I., et al. (2020). High resolution structure-from-motion models and orthophotos of the southern sections of the 2019 Mw 7.1 and Mw 6.4 Ridgecrest earthquakes surface ruptures. Seismological Research Letters 91, 2124-2126, doi: 10.1785/0220190289

Ponti, D. J., et al. (2020). Documentation of Surface Fault Rupture and Ground-Deformation Features Produced by the 4 and 5 July 2019 Mw 6.4 and Mw 7.1 Ridgecrest Earthquake Sequence. Seismological Research Letters 91 (5):